The differential approximation for radiative transfer in an emitting, absorbing and anisotropically scattering medium

ARTICLE *in* JOURNAL OF QUANTITATIVE SPECTROSCOPY AND RADIATIVE TRANSFER · JANUARY 1980

Impact Factor: 2.65 · DOI: 10.1016/S0022-4073(80)80010-0

2 AUTHORS, INCLUDING:

Michael Modest
University of California, Merced

245 PUBLICATIONS **4,323** CITATIONS

SEE PROFILE

J. Quant. Spectrosc. Radiat. Transfer Vol. 23, pp. 117–120
Pergamon Press Ltd., 1980. Printed in Great Britain

NOTE

THE DIFFERENTIAL APPROXIMATION FOR RADIATIVE TRANSFER IN AN EMITTING, ABSORBING AND ANISOTROPICALLY SCATTERING MEDIUM†

M. F. MODEST and F. H. AZAD
Department of Mechanical Engineering, Aeronautical Engineering & Mechanics Rensselaer Polytechnic Institute Troy, NY 12181, U.S.A.

(*Received* 26 *June* 1979)

Abstract—The validity of the well-established differential approximation in radiative transfer is extended to include linear-anisotropic scattering. Sample results demonstrate the accuracy of the method.

OUTLINE OF THEORETICAL CONSIDERATIONS

The differential approximation and its jump boundary conditions for radiative heat transfer has been used successfully for a number of years, but only for non-scattering media[1–3] or isotropically scattering media.[4] It is the purpose of this note to demonstrate that the differential approximation is readily extended to evaluate radiative transfer in anisotropically scattering media.

Consider the equation of transfer

$$\frac{dI_\lambda}{ds} = \mathbf{s}\cdot\nabla I_\lambda = \kappa_\lambda I_{b\lambda} - \beta_\lambda I_\lambda + \frac{\sigma_\lambda}{4\pi}\int_{4\pi} I_\lambda(\mathbf{s}')\Phi_\lambda(\mathbf{s},\mathbf{s}')\,d\omega', \tag{1}$$

where I_λ is the monochromatic intensity, $\mathbf{s}$ is a unit direction vector, κ_λ is the absorption coefficient, σ_λ is the scattering coefficient, and $\beta_\lambda = \kappa_\lambda + \sigma_\lambda$ is the extinction coefficient. The scattering phase function may be expressed as a series in Legendre polynomials,[5]

$$\Phi_\lambda(\mathbf{s},\mathbf{s}') = 1 + \sum_{n=1}^{\infty} a_n P_n(\mathbf{s}\cdot\mathbf{s}'). \tag{2}$$

In an optically thick medium, for which the differential approximation is valid, the intensity can only deviate slightly from an isotropic distribution and may be approximated by[4]

$$I_\lambda \cong \frac{1}{4\pi}(I_{0\lambda} + 3\mathbf{q}_\lambda\cdot\mathbf{s}), \tag{3}$$

where $I_{0\lambda}$ is the solid-angle integrated intensity and $\mathbf{q}_\lambda$ is the radiative heat flux. Multiplying Eq. (1) by 1 and $\mathbf{s}$, respectively, and integrating over all solid angles yields

$$\nabla\cdot\mathbf{q}_\lambda = \kappa_\lambda(4\pi I_{b\lambda} - I_{0\lambda}), \tag{4}$$

$$\nabla I_{0\lambda} = -3\left[\kappa_\lambda + \left(1 - \frac{a_1}{3}\right)\sigma_\lambda\right]\mathbf{q}_\lambda, \tag{5}$$

if Eq. (3) is employed. Equations (4) and (5) constitute the differential approximation together with the boundary condition[4]

$$2\mathbf{q}_\lambda\cdot\mathbf{n} = \frac{\epsilon_\lambda}{2-\epsilon_\lambda}(4\pi I_{b\lambda,w} - I_{0\lambda}), \tag{6}$$

†Supported by the National Science Foundation under NSF Grant ENG 77-12628.

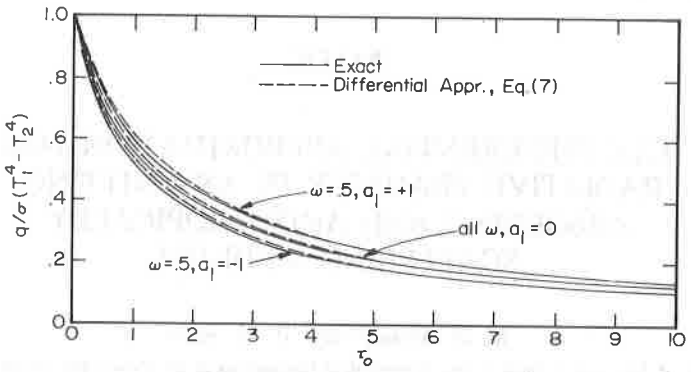

Fig. 1. Nondimensional wall fluxes for radiative equilibrium with anisotropic scattering.

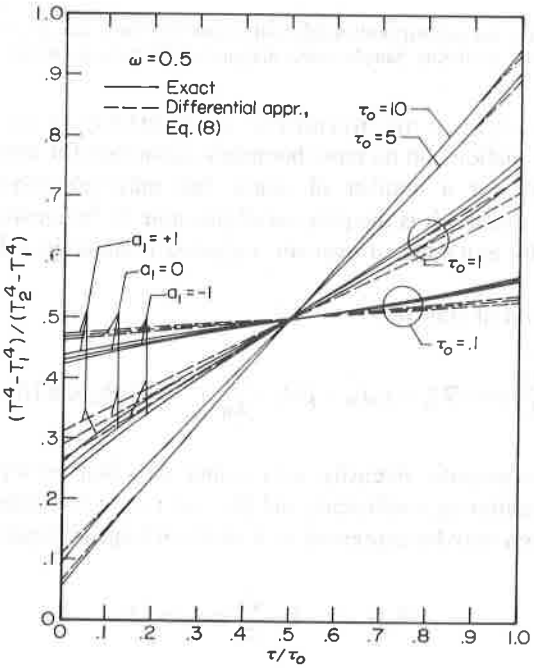

Fig. 2. Nondimensional temperature distribution for radiative equilibrium with anisotropic scattering.

where $\mathbf{n}$ is an outward surface normal, and ϵ_λ is the emissivity of the surface. It should be noted that only the first two terms of Eq. (2) appear in Eqs. (4) and (5), since in a thick medium the intensity becomes "flattened" immediately after scattering. Thus, Mie-scattering phase functions with many terms due to sharp scattering peaks must be approximated by a linear-anisotropic phase function with $|a_1| \leq 1$, in order to avoid negative scattering ($|a_1| > 1$).

SAMPLE RESULTS

In order to demonstrate the accuracy of the differential approximation with anisotropic scattering, a gray, one-dimensional, plane-parallel layer bounded by black walls is considered, with the medium (i) at radiative equilibrium, (ii) at constant temperature (and equal wall temperatures). The solutions to Eqs. (4)–(6) are listed below.

(i) Radiative Equilibrium—

$$\frac{q}{\sigma(T_1^4 - T_2^4)} = \frac{1}{1 + \frac{3}{4}\left(1 - \frac{a_1\omega}{3}\right)\tau_0}, \tag{7}$$

$$\frac{T^4-T_1^4}{T_2^4-T_1^4}=\frac{1}{2}\frac{1+\frac{3}{2}\left(1-\frac{a_1\omega}{3}\right)\tau}{1+\frac{3}{4}\left(1-\frac{a_1\omega}{3}\right)\tau_0}; \tag{8}$$

(ii) Constant Temperature—

$$\frac{q}{\sigma(T^4-T_w^4)}=\frac{2\sinh\left[\sqrt{[(3-a_1\omega)(1-\omega)]}(\tau-\tau_0/2)\right]}{\sinh\left[\sqrt{[(3-a_1\omega)(1-\omega)]}\frac{\tau_0}{2}\right]+\frac{1}{2}\sqrt{\left(\frac{3-a_1\omega}{1-\omega}\right)}\cosh\left[\sqrt{[(3-a_1\omega)(1-\omega)]}\frac{\tau_0}{2}\right]}, \tag{9}$$

where $\omega=\sigma/\beta$ is the single-scattering albedo.

The results for radiative equilibrium are shown in Figs. 1 and 2, and are compared with exact numerical results obtained from the full integral equations. Figure 1 depicts the heat flux

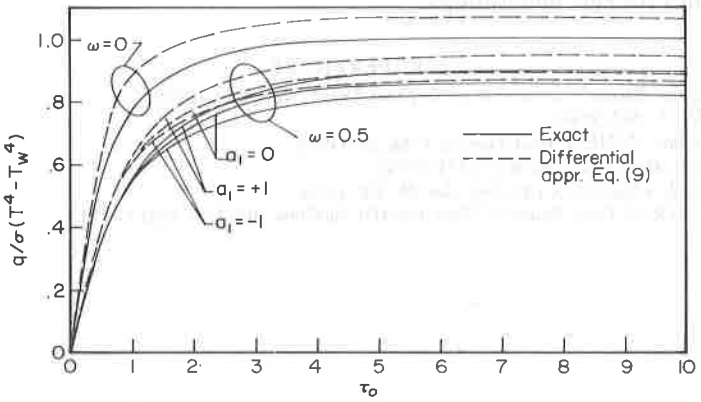

Fig. 3. Nondimensional wall fluxes for constant-temperature slab with anisotropic scattering.

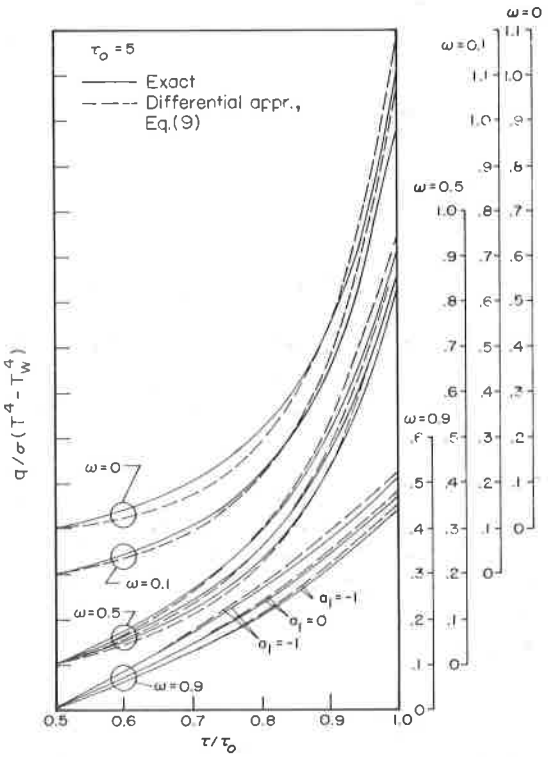

Fig. 4. Nondimensional heat-flux distribution over a constant-temperature slab with anisotropic scattering.

rates between the plates for varying optical thickness for a typical albedo of $\omega = 0.5$. The case of $a_1 = 0$ (isotropic scattering) is valid for any value of ω, as examination of Eq. (7) and of the exact relations[6] shows. Thus, this line in Fig. 1 gives an indication of the accuracy of the differential approximation for non-scattering and isotropically scattering media. It is seen that the accuracy for strong forward-scattering ($a_1 = +1$) and strong backward scattering ($a_1 = -1$) is virtually the same. The same is true for the temperature distribution across the gap depicted in Fig. 2. For larger optical thicknesses ($\tau_0 \geq 5$), anisotropic scattering has only a negligible influence on the temperature distribution and is, therefore, not shown in the graph.

The results for a constant-temperature slab are shown in Figs. 3 and 4. Figure 3 depicts the flux at the walls as a function of optical thickness, showing that the slab virtually becomes a semi-infinite body for optical thicknesses of $\tau_0 \geq 5$. Overprediction of the wall fluxes by the differential approximation is again essentially the same for non-scattering media ($\omega = 0$), isotropic scattering ($a_1 = 0$), and strong forward and backward scattering ($a_1 = \pm 1$). Similar conclusions can be drawn from Fig. 4, which shows local heat fluxes across the slab for a typical optical thickness of $\tau_0 = 5$. It is also seen that the differential approximation is least accurate close to the surface where, especially at large optical thicknesses, the radiation intensity becomes strongly non-isotropic.

REFERENCES

1. A. S. Eddington, *The Internal Constitution of the Stars.* Dover, New York (1959).
2. P. Cheng, *AIAA J.* 2, 1662 (1964).
3. R. G. Deissler, *Trans. ASME, J. Heat Transfer* C-**86**, 240 (1964).
4. M. F. Modest, *Lett. Heat Mass Transfer* 3, 111 (1976).
5. C. M. Chu and S. W. Churchill, *J. Opt. Soc. Am.* **45**, 958 (1955).
6. E. M. Sparrow and R. D. Cess, *Radiation Heat Transfer.* McGraw-Hill, New York (1978).